

RESEARCH ARTICLE



Construction of a novel prognostic model based on lncRNAs-related to DNA damage repair for predicting the prognosis of clear cell renal cell carcinoma

Peng Chen[†], Jian Li[†] and Renli Tian

Department of Urology, General Hospital of Northern Theater Command, Shenyang, Liaoning, China

ABSTRACT

Background: CcRCC has the characteristics of high aggression, high metastasis, high mortality, wide tumour heterogeneity and variable clinical course. The purpose of this study was to explore the potential value of lncRNAs-related to DNA damage repair (DDR) in predicting the prognosis of ccRCC by construction and verification a novel prognostic model.

Methods: RNA-seq data and clinical data of ccRCC were downloaded from public databases. Subsequently, Pearson correlation analysis and differential expression analysis were performed to identify DElncRNAs-related to DDR. Then, through univariate Cox analysis and LASSO analysis, the DElncRNAs-related to DDR associated with prognosis were screened for the construction of novel risk score prognostic model. In addition, functional annotation, tumour mutation burden, immune correlation and drug sensitivity analyses were performed based on risk score to assess the characteristics of patients in different risk score groups.

Results: Based on univariate Cox analysis and LASSO analysis, four best DElncRNAs-related to DDR were selected. Subsequently, a novel risk score prognostic model based on these four DElncRNAs was constructed through LASSO. Multivariate Cox analysis showed that risk score and age were independent prognostic factors for ccRCC ($p < 0.05$). Functional enrichment analysis showed that DDR-related biological processes were mainly enriched in the high risk group. The highly mutated genes in the high and low risk groups were the same (VHL, PBRM1 and TTN), but they also had their own unique mutated genes. Pearson correlation analysis showed that the risk score was significantly ($p < 0.05$) positively correlated with the infiltration degree of CD8 T cells evaluated by six algorithms. In addition, it was found that the high and low risk groups had different sensitivities to the drugs Etoposide, Imatinib, Sorafenib, Bosutinib and Sunitinib.

Conclusion: A novel prognostic model was constructed based on four DElncRNAs-related to DDR. The model has satisfactory accuracy in predicting survival of ccRCC patients.

ARTICLE HISTORY

Received 16 October 2024

Revised 27 February 2025

Accepted 9 March 2025

KEYWORDS



Clear cell renal cell carcinoma; DNA damage repair; lncRNAs; risk score; survival

Introduction


Clear cell renal cell carcinoma (ccRCC, or KIRC) has a poor prognosis, accounting for about 80% of renal cell carcinoma (RCC), and is also the most notorious subtype of RCC [1,2]. CcRCC has the characteristics of high aggression, high metastasis, high mortality, wide tumour heterogeneity and variable clinical course [3,4]. Surgery is the main treatment for ccRCC [5]. Although early surgical treatment is performed, many patients eventually relapse and develop metastases [6]. Moreover, at the time of diagnosis, metastasis occurred in many patients, limiting the surgical treatment of ccRCC. Despite advances in targeted

therapies, patient outcomes remain poor due to secondary drug resistance [7,8]. Therefore, it is urgent to identify more biomarkers for prognostic evaluation and treatment guidance of ccRCC, and it is necessary to establish a reliable prognostic model to predict clinical outcomes.

Organisms are constantly exposed to numerous DNA damage factors, making the genome constantly threatened by different types of DNA damage. In order to maintain the stability of the genome, powerful DNA repair and damage bypass mechanisms faithfully protect DNA by removing or tolerating damage [9,10]. DNA damage repair (DDR) dysfunction can lead to

CONTACT Renli Tian  tianrenli@aliyun.com  Department of Urology, General Hospital of Northern Theater Command, No. 83, Wenhua Road, Shenyang, Liaoning 110016, China

[†]These authors contributed equally to this work and can be considered as co-first authors.

 Supplemental data for this article can be accessed online at <https://doi.org/10.1080/07853890.2025.2480755>.

© 2025 The Author(s). Published by Informa UK Limited, trading as Taylor & Francis Group

This is an Open Access article distributed under the terms of the Creative Commons Attribution-NonCommercial License (<http://creativecommons.org/licenses/by-nc/4.0/>), which permits unrestricted non-commercial use, distribution, and reproduction in any medium, provided the original work is properly cited. The terms on which this article has been published allow the posting of the Accepted Manuscript in a repository by the author(s) or with their consent.

accumulation of DNA damage, susceptibility to cancer, high sensitivity to chemotherapy and radiotherapy, and is also associated with response to immune checkpoint inhibitors [11]. Defects in the DDR process may lead to various diseases, including tumours. Therefore, the DDR system has emerged as a new target for anti-tumour drugs [12]. Harmful DDR gene alterations are recurrent genomic events in patients with advanced RCC [13]. Regulation of DDR may influence the susceptibility of ccRCC patients to sunitinib [14].

The best function of long non-coding RNAs (lncRNAs) is that they regulate gene and genome activity at different levels [15]. LncRNAs dysregulation plays an important role in cancer and can be used as diagnostic, prognostic, and therapeutic biomarkers [16]. Oncological studies have shown that lncRNAs can affect the formation and prognosis of cancer by affecting mRNAs/miRNAs-related to DDR, including colorectal cancer, non-small cell lung cancer, etc [17–19]. Previous studies have shown that the effects of lncRNAs on ccRCC are multifaceted, including the migration and invasion of cancer cells, the progression and prognosis of diseases [20–22]. However, there is limited research on lncRNAs-related to DDR in ccRCC, and it is not well understood whether they are associated with prognosis. Therefore, it is important to analyze the expression pattern, prognostic value and clinical significance of lncRNAs-related to DDR in ccRCC.

In this study, RNA-seq data and clinical data of ccRCC were downloaded from public databases. Differentially expressed lncRNAs (DELncRNAs)-related to DDR were identified by Pearson correlation analysis and differential expression analysis. Subsequently, a novel prognostic model based on DELncRNAs-related to DDR was constructed. In addition, immune cell infiltration, tumor mutation burden (TMB), and drug sensitivity analysis were also performed. The purpose of this study was to explore the potential value of lncRNAs-related to DDR in predicting the prognosis of ccRCC by construction and verification a novel prognostic model.

Materials and methods

Data source

The RNA-seq data, matched survival information and clinicopathological features of The Cancer Genome Atlas-ccRCC (TCGA-ccRCC) were extracted from the University of California Santa Cruz (UCSC) Xena database (<https://xena.ucsc.edu/>). Patients with no survival information and overall survival (OS) less than 30 days

were excluded. A total of 517 cancer tissue samples and 72 normal tissue samples were included. A total of 18779 mRNA expression matrices and 14831 lncRNA expression matrices were obtained using RNA annotation files in the GENCODE database (<https://www.gencodegenes.org/>). In addition, GSE66272 dataset was downloaded from the Gene Expression Omnibus (GEO) database for model lncRNAs expression validation. The Gene Expression Profiling Interactive Analysis (GEPIA) database was also used to validate the expression of model lncRNAs.

Identification of DELncRNAs-related to DDR in ccRCC

A total of 275 genes-related to DDR (DRGs) were obtained from a previous study [23]. Pearson correlation analysis was used to evaluate the correlation between 275 DRGs and 14831 lncRNAs. The screening criteria for lncRNAs-related to DDR were Pearson |correlation coefficient| > 0.6 and P value (P) < 0.001. The limma in the R package was used to identify DELncRNAs between normal tissues and cancer tissues based on the screening criterion $|\log_2 \text{fold change (FC)}| \geq 1$ and adjusted $p < 0.05$. DELncRNAs-related to DDR were obtained by intersections of lncRNAs-related to DDR and DELncRNAs.

Construction of prognostic risk score model

The dataset containing 517 cancer tissue sample data was randomly divided into a training cohort ($N=258$) and a test cohort ($N=259$) according to 1:1. Univariate Cox analysis ($p < 0.05$) was performed based on the obtained DELncRNAs-related to DDR in the training cohort to screen DELncRNAs-related to DDR with prognostic value. The glmnet in the R package was used to perform LASSO regression analysis to reduce the risk of overfitting and determine the optimal number of DELncRNAs-related to DDR involved in model construction. The risk score formula is $\text{Risk Score} = \sum_{i=1}^n (\text{exp}_i * \beta_i)$ (Note: n, number of lncRNAs; exp_i : expression value of lncRNA i, β_i : regression coefficient of lncRNA i.). Patients were divided into high and low risk groups based on median risk score. Kaplan-Meier analysis was performed using survival and survminer in the R package to compare OS and progression free interval (PFI) between the high and low risk groups ($p < 0.05$). Receiver operating characteristic (ROC) curve analysis was performed by timeROC in the R package to verify the accuracy of the risk model in predicting patients' 1-, 3-, and 5-years survival.

Characteristic analysis of model lncRNAs

The expression difference of model lncRNAs in normal and cancer tissues was analysed based on Wilcoxon test. Patients were divided into high and low expression groups based on the median expression of each model lncRNA. Kaplan-Meier analysis was used to compare the survival differences of patients in the high and low expression groups of model lncRNAs ($p < 0.05$). Pearson correlation was used to analyse the correlation between the expression of each model lncRNA and the risk score. In addition, the differential expression of each model lncRNA at different disease stages was analysed based on the Wilcoxon test ($p < 0.05$).

Risk score model evaluation

Kaplan-Meier analysis was used to analyse the survival differences between patients with high and low risk scores in different clinical feature subgroups ($p < 0.05$). Univariate and multivariate Cox analyses were used to assess prognostic independence of risk scores and clinical features. The rms in the R package was used to draw a nomogram and predict the 1-, 3- and 5-year survival probability of patients based on the total score. The calibration curve was used to evaluate the prediction accuracy of the nomogram model. The ggDCA in the R package was used to perform decision curve analysis (DCA) analysis to evaluate the clinical utility of the nomogram model.

Correlation analysis of immune cells

The IOBR in the R package was used to evaluate the levels of immune cell infiltration in the tumor microenvironment based on six algorithms (CIBERSORT, MCP counter, EPIC, xCell, TIMER and quanTIseq). Pearson correlation was used to analyse the correlation between risk score and immune cells. The GSVA in the R package was used for immune function score analysis to explore immune function activation status in the high and low risk groups.

Identification and functional enrichment of differentially expressed mRNAs (DEmRNAs) in high- and low-risk groups

The limma in the R package was used to identify DEmRNAs between high- and low-risk groups based on $|\log_2 \text{FC}| \geq 1$ and adjusted $p < 0.05$. The clusterProfiler and enrichplot in the R package were used to perform functional enrichment analyses, including

gene ontology (GO) and Kyoto Encyclopedia of Genes and Genomes (KEGG) enrichment analyses. In addition, gene set enrichment analysis (GSEA) was also performed. Adjusted $p < 0.05$ was considered statistically significant.

TMB and medication guidance

Somatic mutation data were downloaded from TCGA. The maftools, survival and survminer in the R package were used to evaluate gene mutations in the high and low risk groups and the diverse survival associated with the TMB score. Subsequently, the expression differences of important immune checkpoints between high and low risk groups were compared based on the Wilcoxon test. Important immune checkpoints were obtained from a previous study [24]. Tumour immune dysfunction and exclusion scores of TCGA-ccRCC samples were obtained based on the TIDE database (<http://tide.dfci.harvard.edu/>) to evaluate the potential clinical efficacy of immunotherapy in different risk groups. The pRRophetic in the R package was used to predict the half maximal inhibitory concentration (IC50) of drugs commonly used in cancer patients.

Validation of model lncRNAs expression in clinical samples

This study was approved by the Ethics Committee of General Hospital of Northern Theater Command (Y(2024)277). Written informed consent was obtained from all participants. The inclusion criteria for ccRCC patients were as follows: (1) Patients were diagnosed with ccRCC for the first time, and all were confirmed by pathological examination; (2) Patients did not receive radiotherapy, chemotherapy, immunotherapy or molecular targeted therapy before diagnosis; (3) Patients without other malignant tumours; (4) Patients without other autoimmune diseases; (5) patients' age was >18 years old. Patients with combination of other malignancies, preoperative adjuvant chemotherapy, radiotherapy or targeted therapy, incomplete clinical data and history of cancer were excluded. A total of 11 ccRCC patients were included. Cancer and paracancerous tissues from ccRCC patients were collected for real-time quantitative polymerase chain reaction (RT-qPCR). FastKing cDNA first strand synthesis kit (TIANGEN, KR116) and SuperReal PreMix Plus (SYBR Green) (TIANGEN, FP205) were used for reverse transcription and fluorescence quantitative detection, respectively. The relative quantitative analysis of data was carried out by $2^{-\Delta\Delta\text{CT}}$ method.

Statistical analysis

The Wilcoxon test was used to statistically analyse the significance of differences between two groups. $p < 0.05$ was considered statistically significant. All statistical analyses in this study were completed in R software. The limma in the R package was used to identify DElncRNAs and DEMRNAs between high and low risk groups based on $|\log_2 FC| \geq 1$ and adjusted $p < 0.05$.

Results

Identification of DElncRNAs-related to DDR in ccRCC

A total of 251 DElncRNAs were identified based on $|\log_2 FC| \geq 1$ and adjusted $p < 0.05$ (Figure 1(A)). Based on Pearson [correlation coefficient] > 0.6 and $p < 0.001$, 5321 lncRNAs-related to DDR was obtained.

Subsequently, taking the intersection of 5321 lncRNAs-related to DDR and 251 DElncRNAs, a total of 128 DElncRNAs-related to DDR were obtained (Figure 1(B,C)).

Construction of risk score model

In the training cohort, 25 DElncRNAs-related to DDR with prognostic value were obtained by univariate Cox analysis based on 128 DElncRNAs-related to DDR (Figure 2(A)). Among them, nine were protective factors and 16 were risk factors. Subsequently, LASSO regression analysis was further performed to screen out the four best DElncRNAs-related to DDR (AP000439.3, CTA-384D8.36, EMX2OS and SNHG1) with prognostic value (Figure 2(B,C)). The coefficients obtained by the LASSO algorithm were used to calculate the risk score for each tumour sample. The risk score formula is Risk

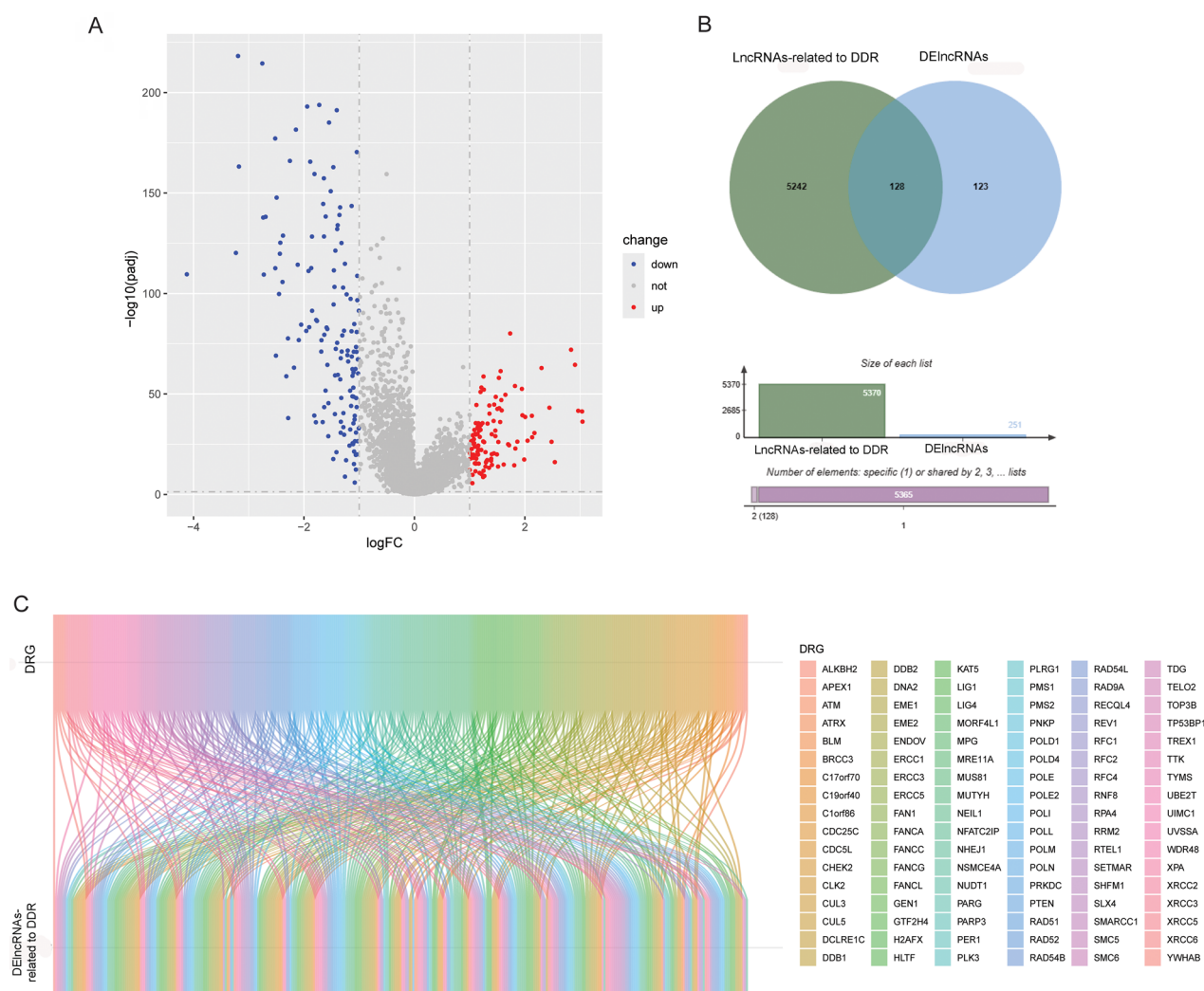


Figure 1. Identification of DElncRNAs related to DDR.

A: Volcanic map of DElncRNAs between normal and cancer tissues; B: Venn diagram of lncRNAs-related to DDR and DElncRNAs; C: Relationship diagram between DRG and DElncRNAs-related to DDR.

Score = $(-0.0940 \times \text{AP000439.3}) + (0.2269 \times \text{CTA-384D8.36}) + (-0.3475 \times \text{EMX2OS}) + (0.0137 \times \text{SNHG1})$.

Patients were divided into high- and low-risk groups based on median risk score (Figure 2(D)). The mortality rate of high risk group was significantly higher than that of low risk group (Figure 2(E)). Heatmap results showed that model lncRNAs AP000439.3 and EMX2OS were low expressed in high-risk group, while CTA-384D8.36 and SNHG1 were high expressed in high-risk group (Figure 2(F)). Kaplan–Meier analysis showed that the low-risk group had a better survival advantage than the high risk group (Figure 2(G)), and PFI also showed a similar trend (Figure 2(H)). ROC results showed that the area under curve (AUC) for 1, 3 and 5 years was 0.737, 0.695 and 0.758, respectively (Figure 2(I)), indicating that the risk model had a good

prognostic prediction accuracy. Based on the same formula, a series of verifications were performed in the test cohort (Supplementary Figure 1 (A–G)) and the entire cohort (Supplementary Figure 1 (H–N)), and the results were consistent with the training cohort. The results of principal component analysis (PCA) showed that the samples in each cohort could be clearly divided into high- and low-risk groups (Figure 2(J) and Supplementary Figure 1 (G and N)).

Characteristic analysis of model lncRNAs

Compared with normal tissues, AP000439.3, CTA-384D8.36 and SNHG1 were up-regulated in cancer tissues, while EMX2OS was down-regulated in cancer tissues (Figure 3(A)). Kaplan–Meier analysis showed

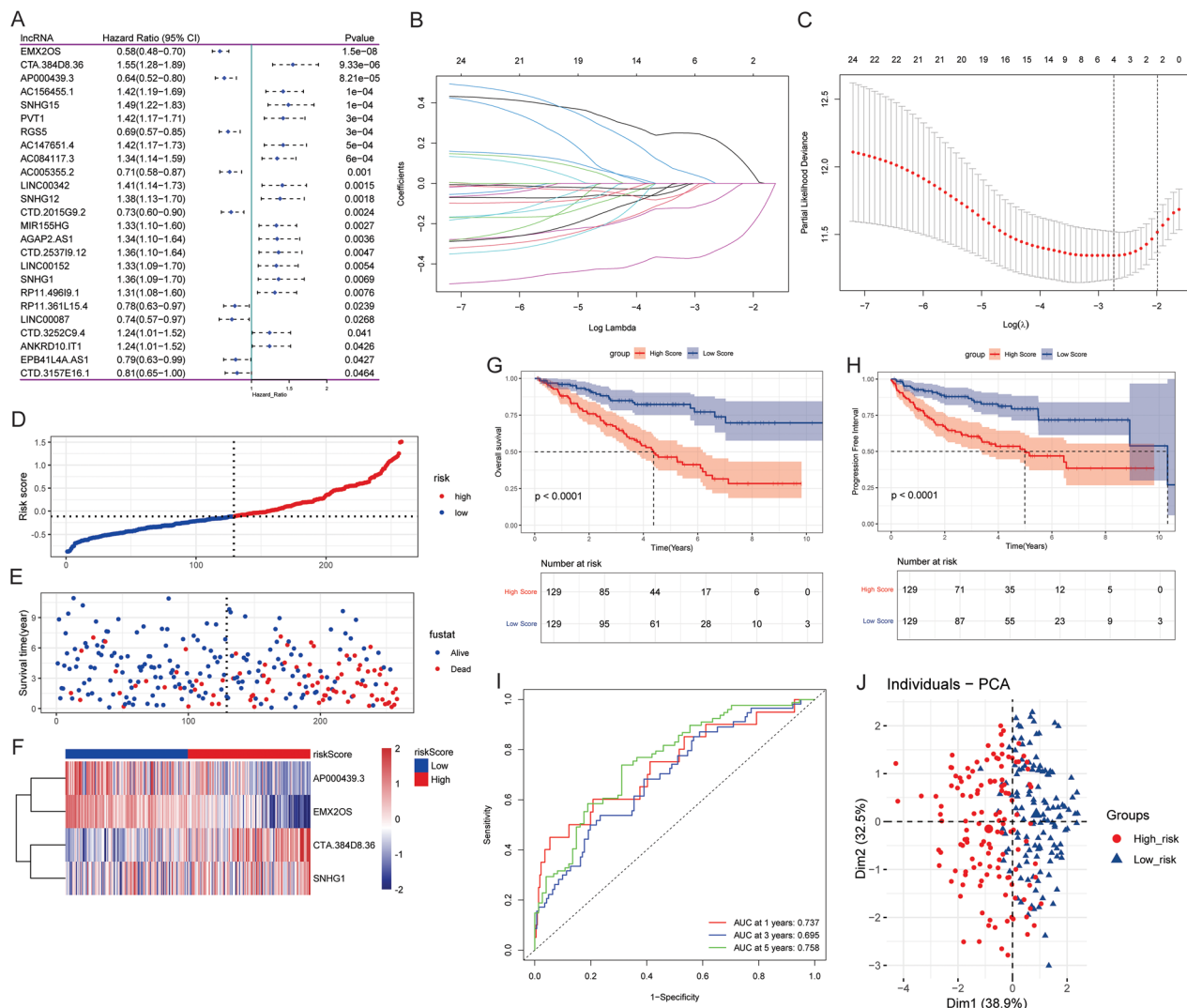


Figure 2. Construction of risk score model in the training cohort.

A: The forest plot of prognosis-related DElncRNAs related to DDR; B: The process of reducing the number of variables and adjusting coefficients in LASSO regression model; C: Selection of the optimal parameter (lambda) in the LASSO model; D-F: Distribution of risk score and survival status, and heatmap for four model lncRNAs in the training cohort; G: Kaplan–Meier analysis curve for OS of patients in high- and low-risk groups; H: Kaplan–Meier analysis curve for PFI of patients in high- and low-risk groups; I: Time dependent ROC curves for 1-, 3- and 5-years; J: PCA of patients in high- and low-risk groups.

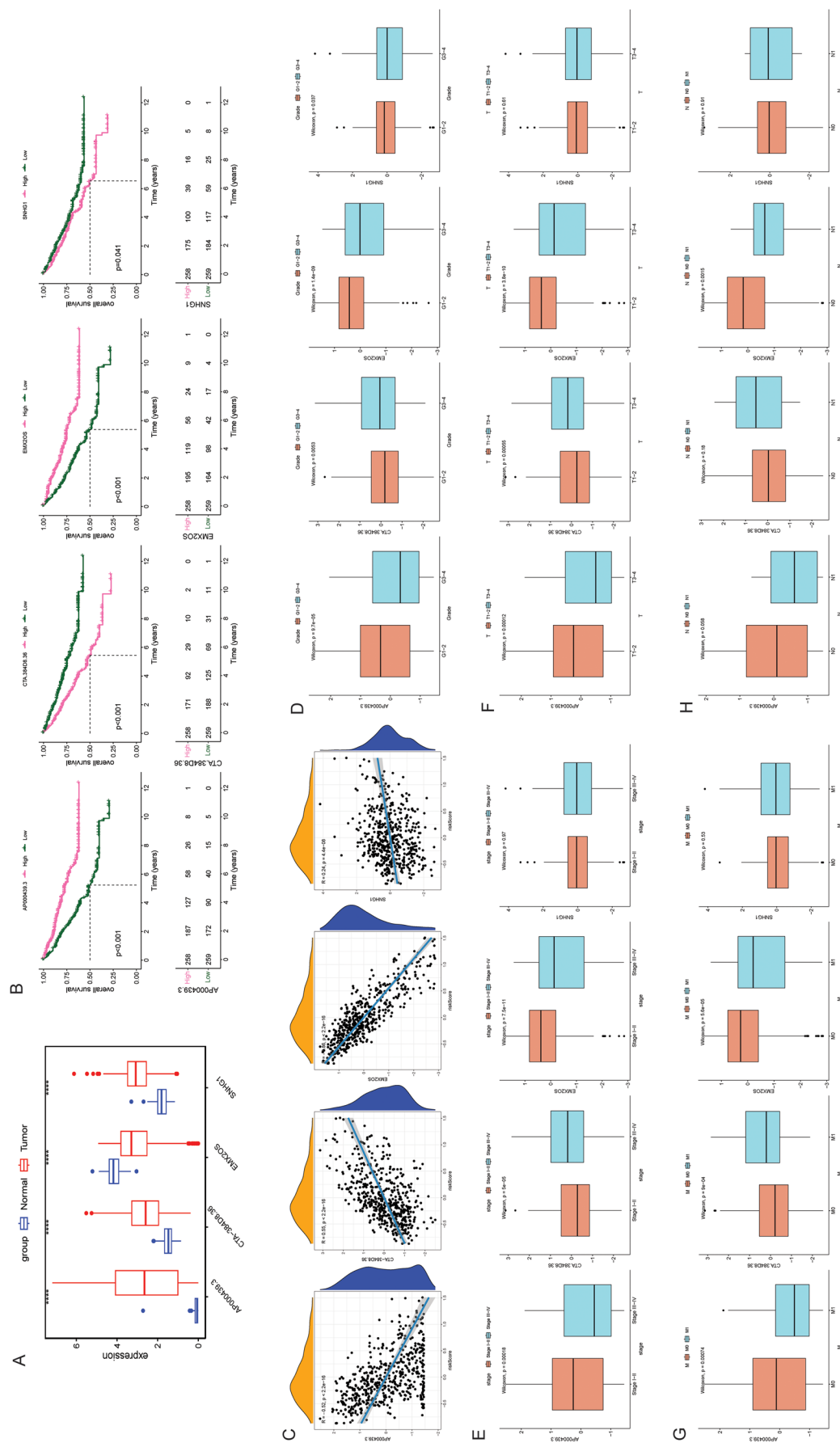


Figure 3. Characteristic analysis of model lncRNAs in the entire cohort.

A: Differential expression box plots of AP000439.3, CTA-384D8.36, EMX2OS and SNHG1 in normal and cancer groups; B: Kaplan-Meier analysis curves for OS of patients in high and low expression groups; C: Correlation between model lncRNAs expression and risk score; D: Differential expression box plots of model lncRNAs in different grade stage groups; E: Differential expression box plots of model lncRNAs in different T stage groups; F: Differential expression box plots of model lncRNAs in different M stage groups; G: Differential expression box plots of model lncRNAs in different N stage groups; H: Differential expression box plots of model lncRNAs in different N stage groups.

that patients with low expression of AP000439.3 and EMX2OS had poor prognosis, and their expression was negatively correlated with risk score. Patients with high expression of CTA-384D8.36 and SNHG1 had poor prognosis, and their expression was positively correlated with risk score (Figure 3(B,C)). Subsequently, the differential expression of four model lncRNAs in different grade, stage, T, M and N stages was analysed. The results showed that the expression of AP000439.3 and EMX2OS was lower in late stage patients, while the expression of CTA-384D8.36 was higher (Figure 3(D-H)), indicating that AP000439.3, EMX2OS and CTA-384D8.36 may mediate the progression of ccRCC. Moreover, low expression of EMX2OS may also cause lymphatic metastasis of ccRCC (Figure 3(H)).

Clinical features and risk score

The survival outcomes of patients in the low risk group were significantly better than those in the high risk group in different age, gender, grade stage, M stage, T stage and stage subgroups (Figure 4(A-F)). Moreover, the survival outcomes of patients in the low-risk group of stage N0 without lymphatic metastasis were also better than those in the high-risk group, but there was no significant difference between the two groups in stage N1 with lymphatic metastasis (Figure 4(G)). Univariate Cox analysis showed that risk score, age, grade stage, stage, M stage, N stage and T stage were risk factors for ccRCC ($p < 0.05$) (Figure 5(A)). Multivariate Cox analysis showed that risk score and age were independent

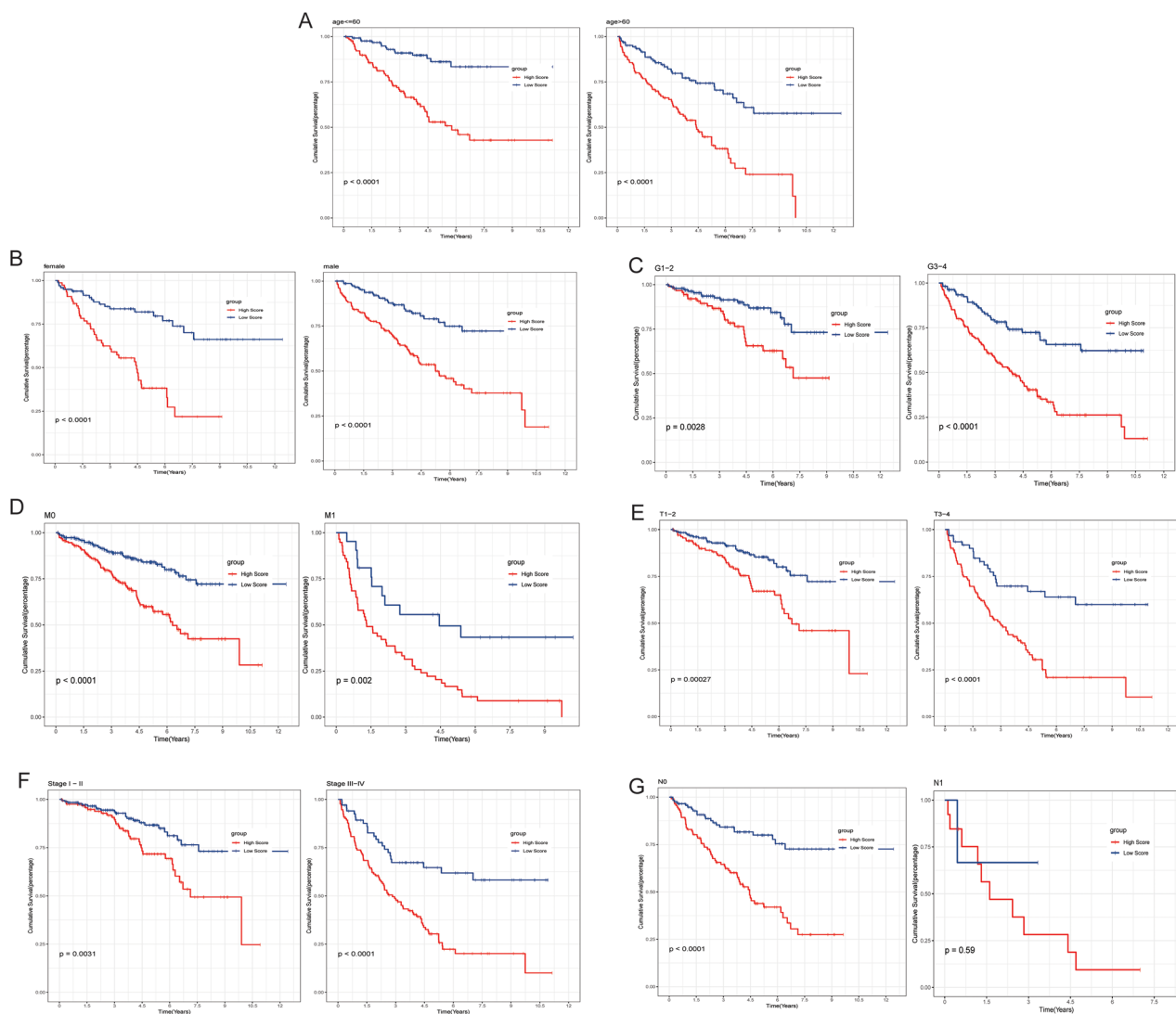


Figure 4. Kaplan–Meier analysis curves for survival of patients with high- and low-risk scores in different subgroups of clinical features. A: Kaplan–Meier analysis curves for survival of patients with high- and low-risk scores in different age groups; B: Kaplan–Meier analysis curves for survival of patients with high- and low-risk scores in different gender groups; C: Kaplan–Meier analysis curves for survival of patients with high- and low-risk scores in different grade stage groups; D: Kaplan–Meier analysis curves for survival of patients with high and low risk scores in different M stage groups; E: Kaplan–Meier analysis curves for survival of patients with high- and low-risk scores in different T stage groups; F: Kaplan–Meier analysis curves for survival of patients with high- and low-risk scores in different stage groups; G: Kaplan–Meier analysis curves for survival of patients with high- and low-risk scores in different N stage groups.

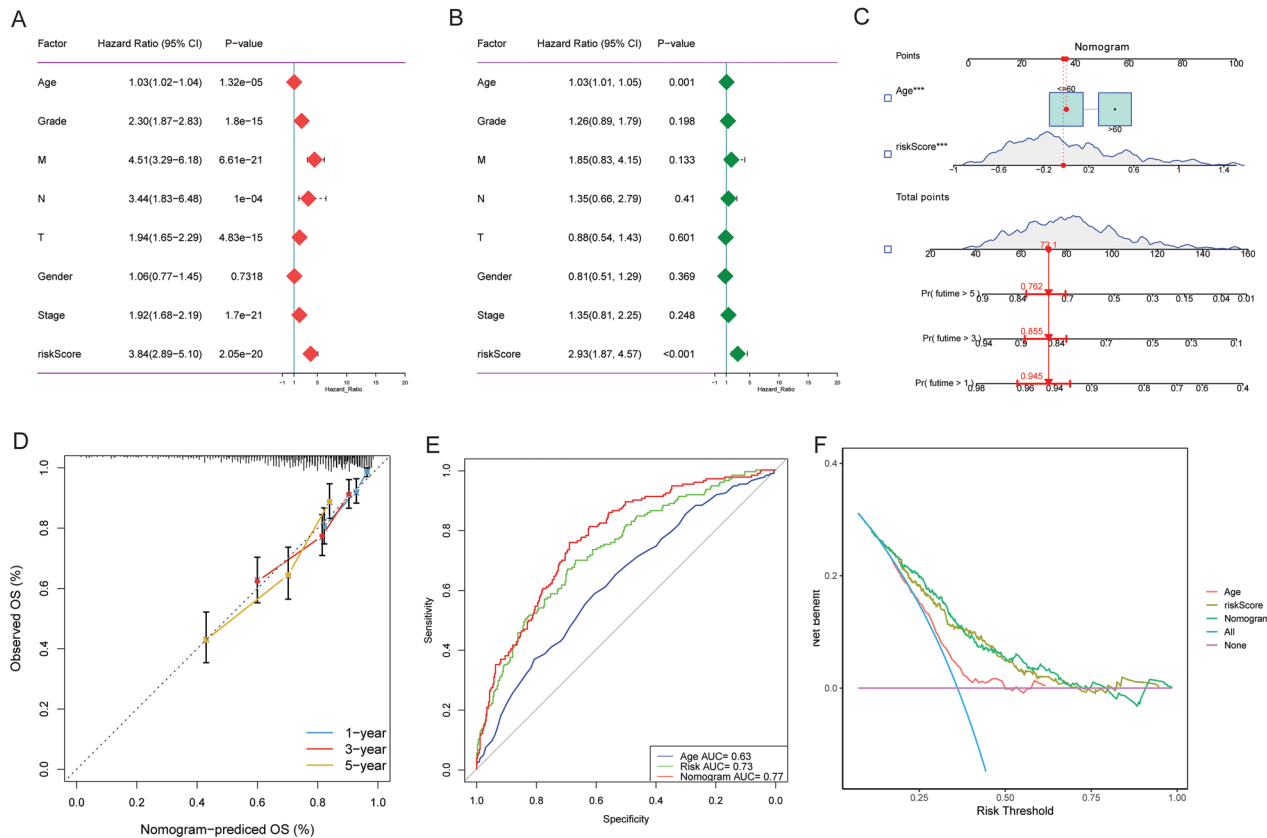


Figure 5. Independent prognostic analysis and nomogram.

A: Univariate Cox regression analysis of risk score and clinical features; B: Multivariate Cox regression analysis of risk score and clinical features; C: A nomogram predicting 1-, 3- and 5-year survival; D: Calibration curve of the nomogram model; E: ROC curves of age, risk score and nomogram; F: DCA curve.

prognostic factors for ccRCC ($p < 0.05$) (Figure 5(B)). Significant variables in multivariate Cox analysis were included in the nomogram model to predict the 1-, 3-, and 5-year survival of patients (Figure 5(C)). The calibration curve showed that the nomogram model had good prognostic prediction ability (Figure 5(D)). ROC curves were used to assess the predictive accuracy of age, risk score and nomogram model. The results showed that the AUC of the age, risk score and nomogram model were 0.63, 0.73 and 0.77, respectively (Figure 5(E)), which indicated that the accuracy of the nomogram was higher. Moreover, the results of decision curve analysis (DCA) also showed that the nomogram model was more effective in the clinical benefit of patients (Figure 5(F)).

Identification and functional enrichment of DEmRNAs in high- and low-risk groups

A total of 86 DEmRNAs were identified between the high- and low-risk groups based on $|\log_2 \text{FC}| \geq 1$ and adjusted $p < 0.05$ (Figure 6(A)). Subsequently, GO and KEGG functional enrichment were performed on DEmRNAs. The functional enrichment results showed that DEmRNAs were enriched in different functions

and pathways, mainly involving transport, metabolic processes, inflammatory responses and other pathways (Figure 6(B,C)). The top five GSEA enrichment processes in the low- and high-risk groups were shown in Figure 6(D,E). Moreover, it was also observed that DDR-related biological processes (e.g. double-strand break repair *via* homologous recombination, homologous recombination and reciprocal homologous recombination) were mainly enriched in the high-risk group (Figure 6(F-H)).

TMB and risk score

The waterfall diagram of somatic mutation distribution showed that the highest mutation gene in the low- and high-risk group was VHL, followed by PBRM1 and TTN (Figure 7(A,B)). Although the two groups of highly mutated genes were consistent, they also have their own unique mutant genes. For example, ATM and DNAH9 were the specific mutated genes of the low-risk group, and FLG and XIRP2 were the specific mutated genes of the high-risk group. The TBM score of the high-risk group was significantly higher than that of the low-risk group (Figure 7(C)). According to the

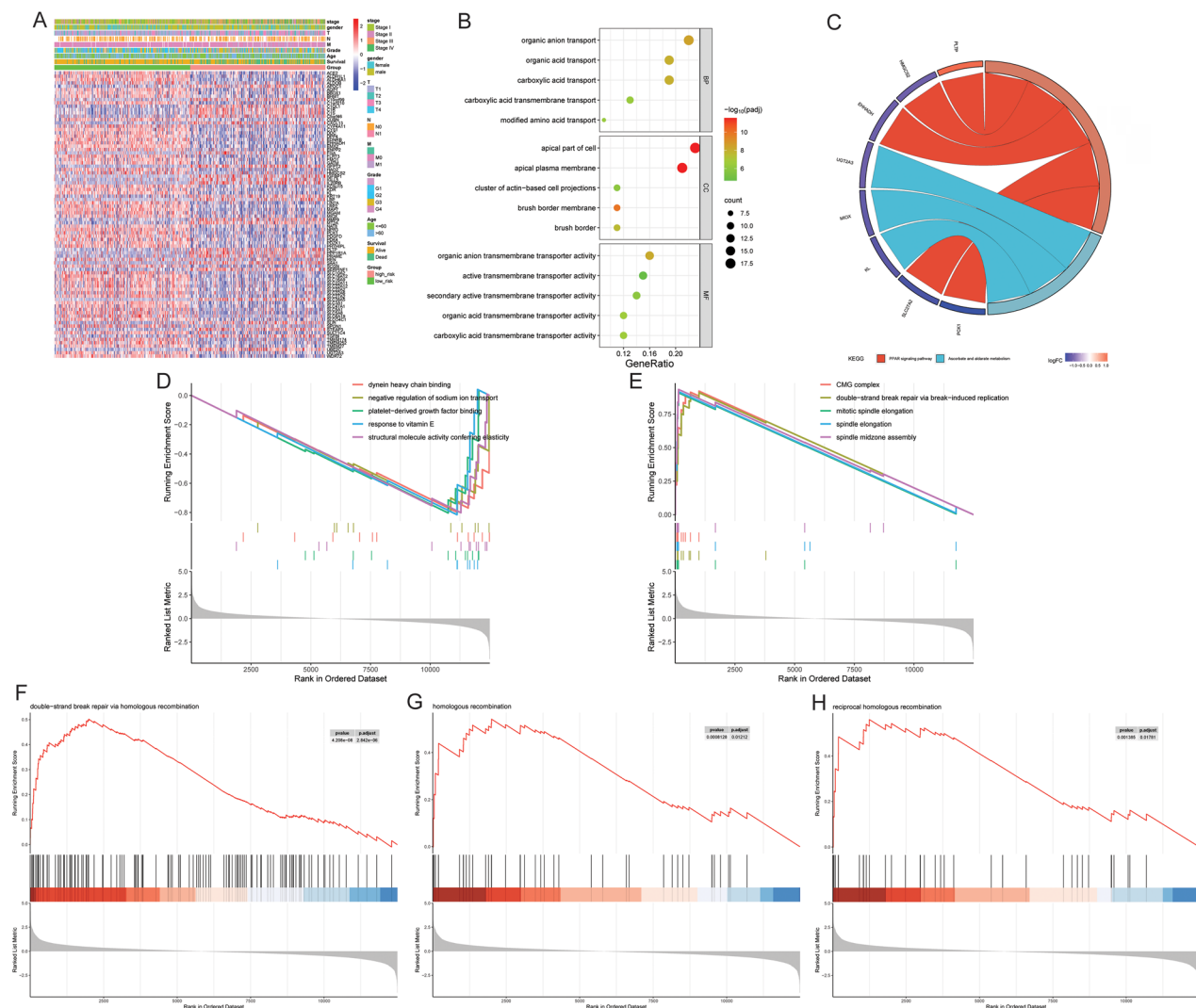


Figure 6. Identification and functional enrichment of DEMrNAs in high- and low-risk group.

A: Heatmap of DEMrNAs between high- and low-risk group; B: Bubble map of GO enrichment analysis of DEMrNAs; C: Circle map of KEGG enrichment analysis of DEMrNAs; D: GSEA enrichment of low-risk group; E: GSEA enrichment of high-risk group; F: GSEA analysis showed that double-strand break repair via homologous recombination was up-regulated in high-risk group; G: GSEA analysis showed that homologous recombination was up-regulated in high-risk group; H: GSEA analysis showed that reciprocal homologous recombination was up-regulated in high-risk group.

median TMB score, the samples were divided into high and low TMB groups. Kaplan–Meier analysis showed that the survival of patients in the low TMB group was significantly better than that in the high TMB group (Figure 7(D)). Combining TMB and risk score to evaluate prognosis, the results showed that low risk and low TMB patients had the best prognosis, while high risk and high TMB patients had the worst prognosis (Figure 7(E)).

Immune landscape and medication guidance

The infiltration level of immune cells in the tumour microenvironment of ccRCC patients was evaluated by six algorithms, and the correlation with the risk score was analysed (Figure 8(A)). Pearson correlation analysis showed that the risk score was significantly ($p < 0.05$)

positively correlated with the infiltration degree of CD8 T cells evaluated by CIBERSORT (correlation coefficient = 0.189), MCP counter (correlation coefficient = 0.320), EPIC (correlation coefficient = 0.279), xCell (correlation coefficient = 0.373), TIMER (correlation coefficient = 0.129) and quantIseq (correlation coefficient = 0.289). Subsequently, CIBERSORT results showed that the degree of multiple immune cell infiltration was significantly different between the high- and low-risk groups (Figure 8(B)), suggesting that the degree of immune cell infiltration may affect the prognosis of patients. In addition, significant differences in immune function activity were found between the high- and low-risk groups (Figure 8(C)). Most immune functions are more active in the high-risk group. Immune checkpoint difference analysis showed that 35key immune checkpoints were significantly different between the high- and low-risk groups

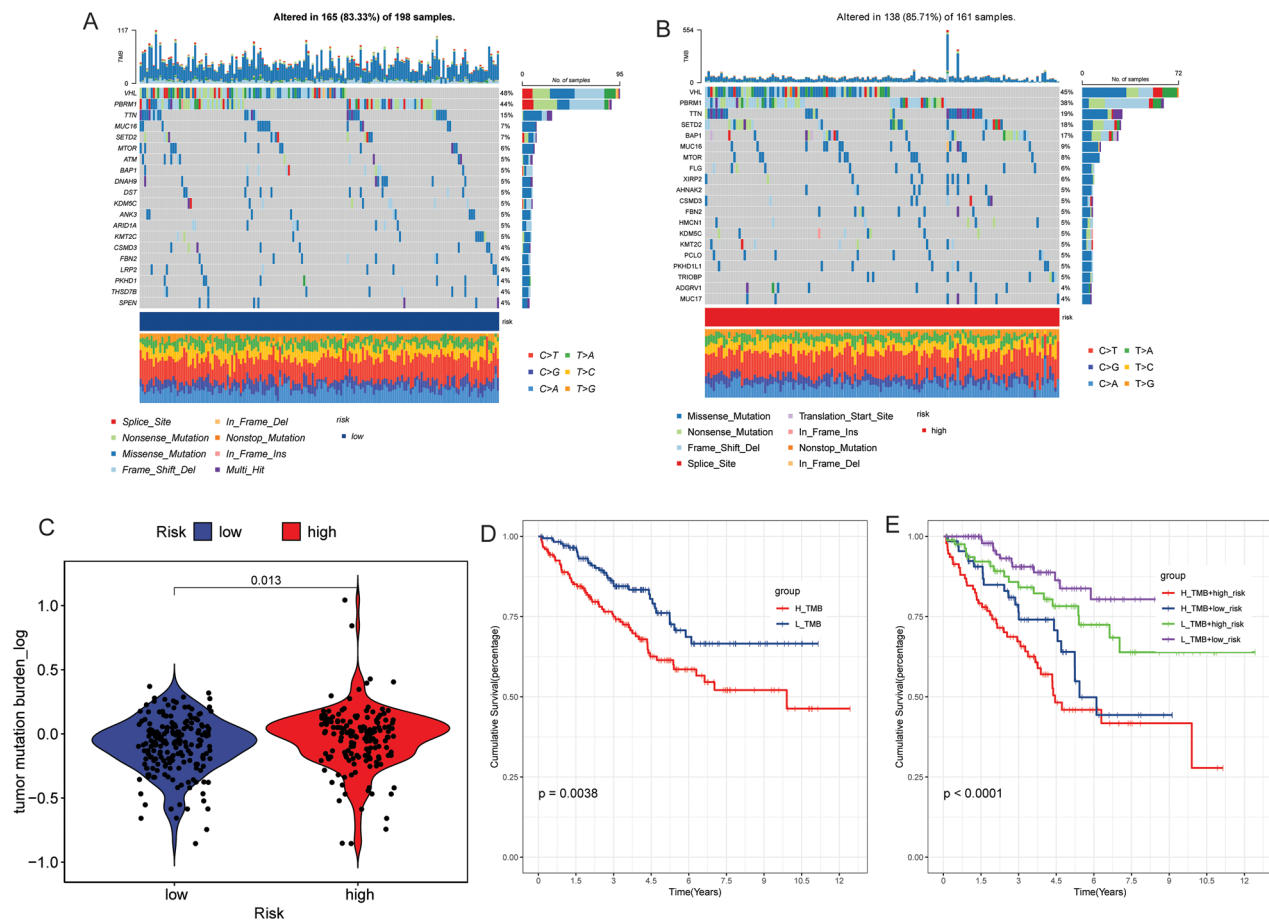


Figure 7. TMB and risk score.

A: Waterfall diagram of somatic mutations in low-risk group; B: Waterfall diagram of somatic mutations in high-risk group; C: The difference of TMB score between high- and low-risk groups; D: Kaplan–Meier analysis curve for survival of patients in high and low TMB groups; E: Kaplan–Meier analysis curve for survival of patients in high TBM+high risk, high TBM+low risk, low TBM+high risk and low TBM+low-risk groups.

(Figure 9(A)), indicating that the risk score may guide immunotherapy medication. Furthermore, the high-risk group also had a higher TIDE score (Figure 9(B)), indicating that the high-risk group had a higher possibility of immune escape and a lower possibility of benefiting from immunotherapy. Subsequently, IC50 values for common drugs in the high- and low-risk groups were calculated. The results showed that the low-risk group was more sensitive to Etoposide, Imatinib and Sorafenib (Figure 9(C–E)), indicating that these drugs may have a better therapeutic effect on patients in the low-risk group. The high-risk group was more sensitive to Bosutinib and Sunitinib (Figure 9(F,G)), indicating that these drugs may have a better therapeutic effect on patients in the high-risk group.

Verification of AP000439.3, CTA-384D8.36, EMX2OS and SNHG1 expression

The expression of model lncRNAs AP000439.3, CTA-384D8.36, EMX2OS and SNHG1 were verified by RT-qPCR (Figure 10). All primers are shown in Table S1.

The results of RT-qPCR showed that the expression trends of CTA-384D8.36, EMX2OS and SNHG1 were consistent with the expression trends in the TCGA-ccRCC dataset. The trend of AP000439.3 expression was contrary to the analysis results in the TCGA-ccRCC dataset, which may be caused by the small sample size of RT-qPCR and sample heterogeneity. In addition, differences in experimental techniques, patients' genetic background and lifestyle habits will also affect the results. Therefore, it is necessary to continue to collect samples to expand the sample for further verification. The expression of model lncRNAs were also validated in the GSE66272 (Supplementary Figure 2A) and GEPIA (Supplementary Figure 2B–E). The results showed that the expression trends of model lncRNAs were consistent with that in the TCGA-ccRCC dataset.

Discussion

LncRNAs are regulatory factors of cellular mechanisms that are often dysregulated in malignant tumors of the genitourinary system [25]. In this study, a novel risk score

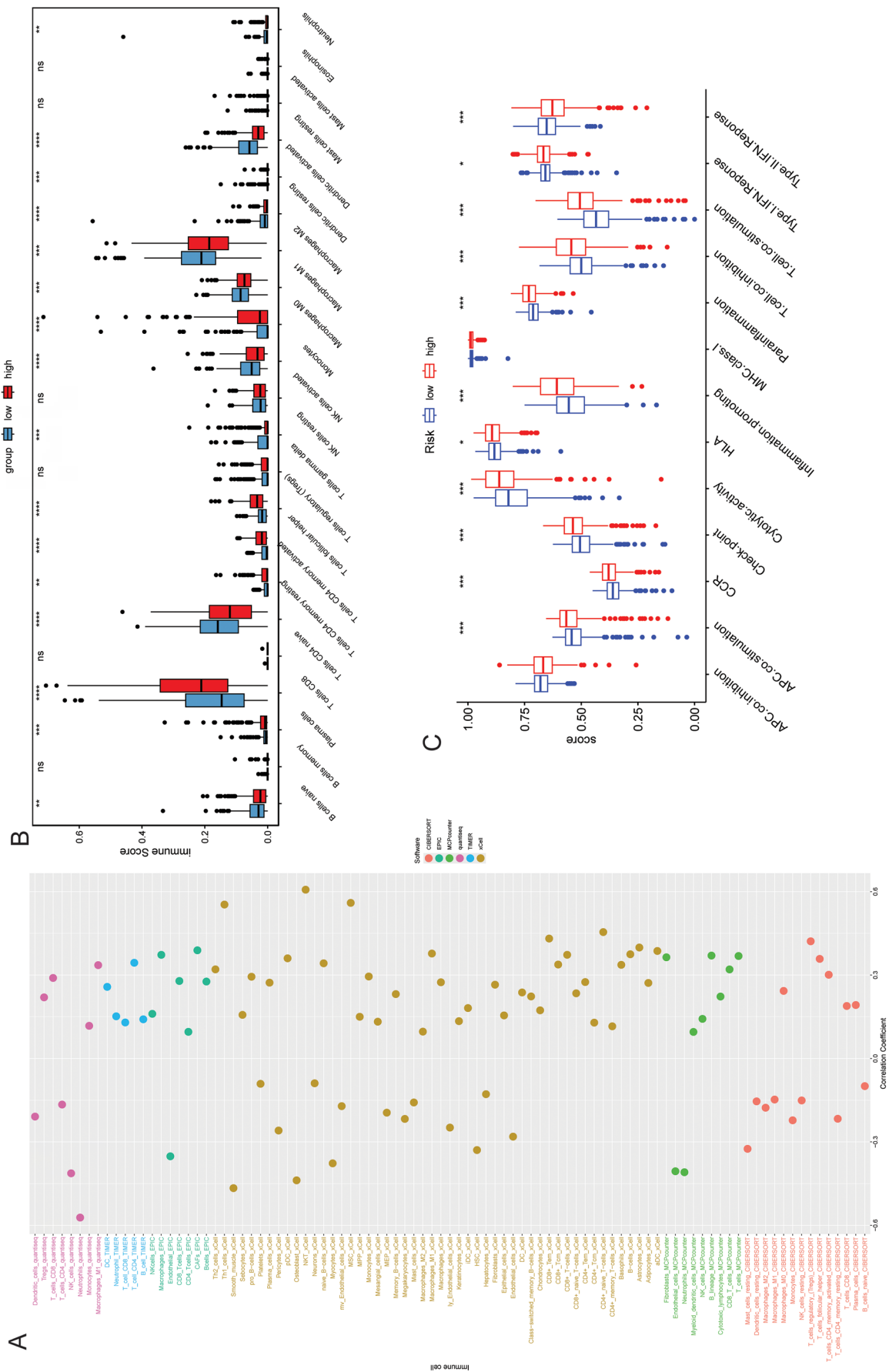


Figure 8. Immune landscape analysis.
 A: Correlation between immune cells and risk score; B: CIBERSORT analysis of immune cell infiltration in high- and low-risk group; C: Box plots of immune-related function difference analysis between high- and low-risk group.

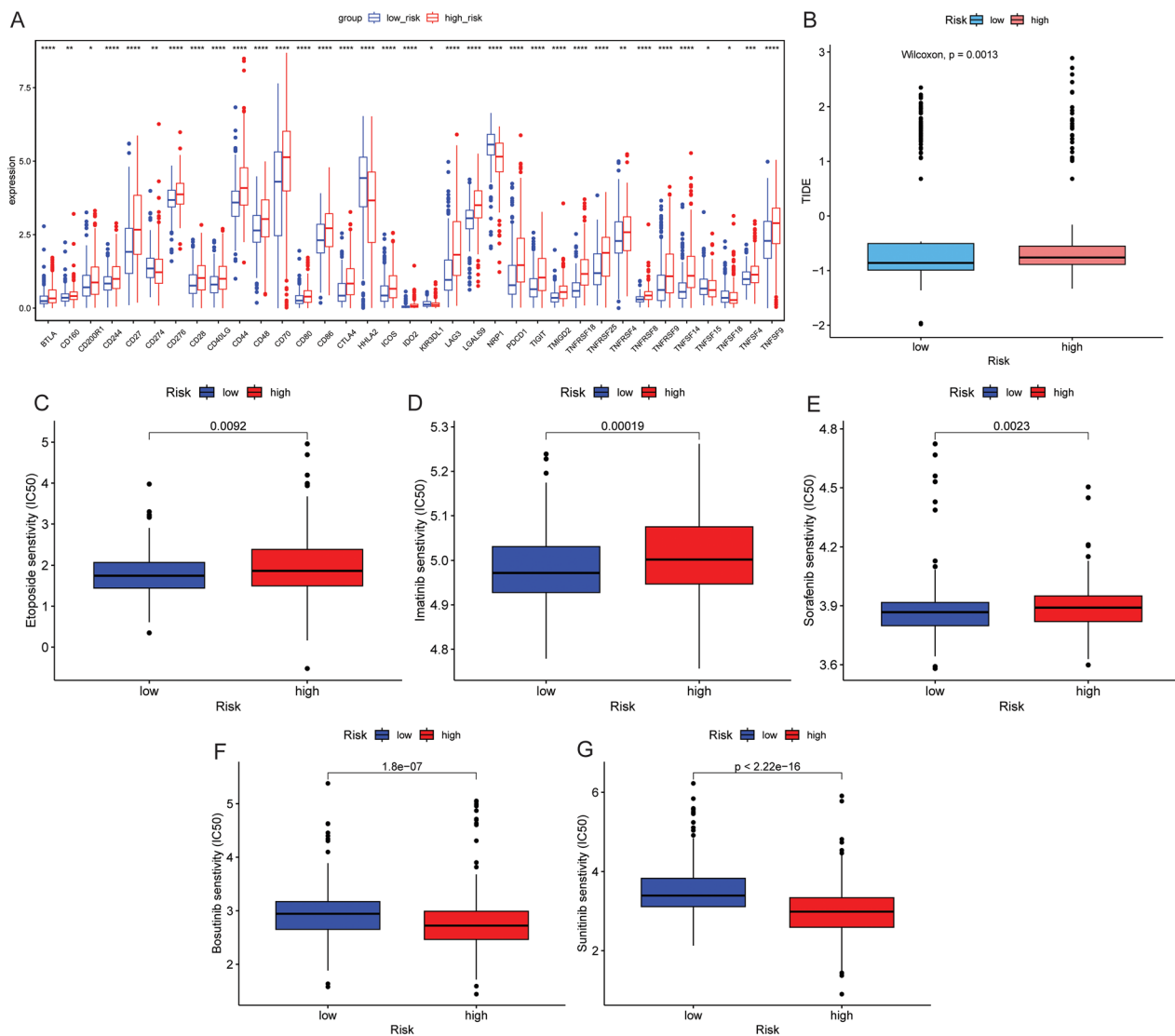


Figure 9. Immune checkpoint and common drug IC₅₀ analyses in high- and low-risk group.

A: Differential expression box plots of 35 key immune checkpoints in high- and low-risk groups; B: Differences of TIDE score between high- and low-risk groups; C: IC₅₀ differences of Etoposide between high- and low-risk groups; D: IC₅₀ differences of Imatinib between high- and low-risk groups; E: IC₅₀ differences of Sorafenib between high and low risk groups; F: IC₅₀ differences of Bosutinib between high and low risk groups; G: IC₅₀ differences of Sunitinib between high- and low-risk groups.

model was constructed based on four DElncRNAs-related to DDR (AP000439.3, CTA-384D8.36, EMX205 and SNHG1). The model has satisfactory accuracy (AUC all above 0.6 in training, test and entire cohorts) in predicting the 1-, 3- and 5-year survival of ccRCC patients. The survival outcomes of patients in the low-risk group were significantly better than those in the high-risk group in different age, gender, grade stage, M stage, T stage and stage subgroups. These results indicate that the risk score can be used to evaluate the prognosis of different subgroups of patients. Multivariate Cox analysis showed that risk score and age were independent prognostic factors for ccRCC. The nomogram model was constructed by combining age and risk score, which further improved the predictive efficacy (AUC = 0.77).

AP000439.3 is highly expressed in ER⁺ breast cancer tissues and is involved in the regulation of cancer cell proliferation and cell cycle progression [26]. AP000439.3 is associated with ccRCC prognosis and is a protective factor [27]. In cancer, certain molecules may be highly expressed due to various mechanisms. However, not all highly expressed molecules imply a poor prognosis. On the contrary, high expression of some molecules may improve patient survival by promoting certain prognostically favourable biological processes (e.g. apoptosis, inhibition of immune evasion, etc.). One study showed that CXCL11 expression is up-regulated in colon adenocarcinoma (COAD), but up-regulated of CXCL11 mRNA is associated with a better prognosis in COAD [28]. In addition, studies have shown that CXCL1

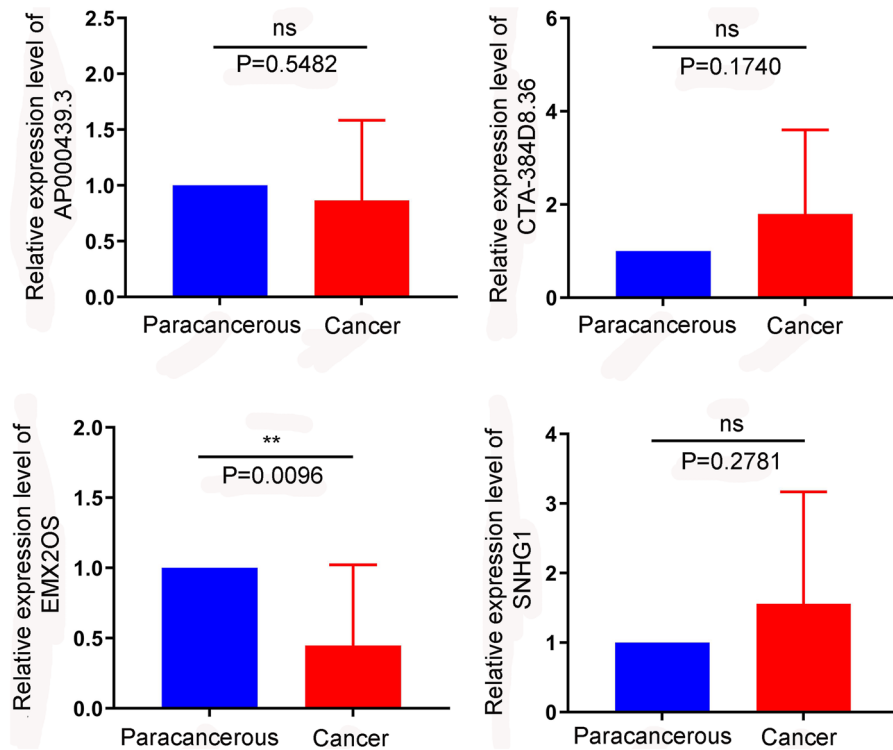


Figure 10. Verification of AP000439.3, CTA-384D8.36, EMX2OS and SNHG1 expression by RT-qPCR.

is highly expressed in colon and gastric cancer and is associated with better prognosis [29,30]. Herein, although AP000439.3 is highly expressed in cancer tissues, its up-regulation is associated with a better prognosis. The expression level of AP000439.3 in different stages of cancer was further analysed, and the results showed that the expression level of AP000439.3 was lower in late-stage patients. These results indicate that AP000439.3 is not only involved in the occurrence of ccRCC, but also related to the progression of ccRCC, and its complex regulatory mechanism deserves further study. So far, no relevant studies on CTA-384D8.36 have been found. To our knowledge, this study is the first to report the potential value of CTA-384D8.36 in ccRCC. EMX2 is essential for urogenital development, and EMX2OS is its antisense transcript [31]. EMX2OS has been reported to be a prognostically protective indicator for ccRCC patients [32,33]. EMX2OS may be a potential therapeutic target for ccRCC, and its down-regulation is significantly associated with higher histological grade, late stage, and poorer prognosis [34]. EMX2OS also participates in regulating the proliferation, migration, and invasion of prostate cancer cells [35]. SNHG1 is a crucial member of the SNHG family. Its expression is up-regulated in a variety of cancers and has great application prospects in the diagnosis, treatment and prognosis of malignant tumours [36]. Studies have shown that SNHG1 is also

involved in the immune escape of RCC and breast cancer [37,38]. In addition, SNHG1 is also involved in the regulation of RCC progression and metastasis [39]. The up-regulated SNHG1 is associated with poor prognosis of RCC patients and affects sunitinib resistance and autophagy of RCC cells [40]. In this study, compared with normal tissues, CTA-384D8.36 and SNHG1 were up-regulated in cancer tissues, while EMX2OS was down-regulated in cancer tissues. Furthermore, CTA-384D8.36, SNHG1, and EMX2OS are associated with prognosis, and CTA-384D8.36 and SNHG1 are involved in regulating ccRCC progression. Moreover, low expression of EMX2OS may cause lymphatic metastasis of ccRCC. Therefore, the risk model of ccRCC constructed by these 4 DElncRNAs-related to DDR has potential reliability.

DDR mechanism is an important safeguard for cells to maintain genomic stability under normal circumstances. When cells are affected by various endogenous and exogenous factors, leading to DNA damage, the DDR mechanism can be promptly activated to recognize and repair these damages, thereby avoiding the accumulation of gene mutations and chromosomal abnormalities and playing a role in inhibiting cancer occurrence [41]. In cancer cells, the DDR mechanism may be abnormal. To meet the needs of their rapid proliferation, tumor cells may over-activate certain DDR pathways, thereby helping tumor cells resist the

DNA damage caused by chemotherapy, radiotherapy, and other treatment methods, leading to drug resistance in tumor cells [42,43]. In addition, the abnormality of the DDR mechanism may also lead to incorrect repairs, resulting in new gene mutations and chromosomal aberrations, which further promote the development and evolution of tumours [44]. In this study, functional enrichment analysis showed that DDR-related biological processes (for example, double-strand break repair *via* homologous recombination, homologous recombination and reciprocal homologous recombination) were mainly enriched in the high-risk group. Moreover, the survival outcomes of patients in the low-risk group were significantly better than those in the high-risk group. Therefore, we speculate that there may be over-activation of DDR in the high-risk group that promotes cancer progression, but the specific situation needs further study.

The highly mutated genes in the high and low risk groups were the same, but they also had their own unique mutated genes. ATM and DNAH9 were the specific mutated genes of the low risk group, and FLG and XIRP2 were the specific mutated genes of the high risk group. ATM is a serine/threonine protein kinase that is recruited by DNA double strand breaks [45]. ATM, DNAH9 and XIRP2 were shown to be mutated in ccRCC patients in previous study [13,46,47]. FLG mutation plays an important role in promoting the development of bladder cancer [48]. This study is the first to report the mutation of FLG in ccRCC. The differences in genes expression and mutation between high- and low-risk group provide new ideas for exploring the molecular mechanism of disease.

Correlation analysis showed that the risk score was positively correlated with the infiltration degree of CD8 T cells. CIBERSORT results showed that CD8 T cells had a higher degree of infiltration in the high-risk group. CD8 T cells are generally cytotoxic and beneficial in many cancers, but their impact in ccRCC depends on their functional state and the tumour microenvironment [49]. Research findings suggest that the infiltration of CD8 T cells within tumours can serve as a prognostic indicator for ccRCC, and is associated with unfavourable clinical outcomes [50,51]. Immune checkpoint blockade and tumour microenvironment-modulating drug treatment were found to benefit ccRCC patients with more infiltrating CD8 T cells [49,52]. There were also significant differences in the expression levels of immune checkpoints between the high- and low-risk groups, indicating that the risk score may guide immunotherapy medication. Therefore, the difference in TIDE scores between high- and low-risk group was also evaluated. The results showed that TIDE scores were higher in the

high-risk group, indicating that the high-risk group had a higher possibility of immune escape and a lower possibility of benefiting from immunotherapy.

In this study, it was found that the high and low-risk groups had different sensitivities to the drugs Etoposide, Imatinib, Sorafenib, Bosutinib and Sunitinib was different. The low-risk group was more sensitive to Etoposide, Imatinib and Sorafenib, while the high risk group was more sensitive to Bosutinib and Sunitinib. Etoposide is a topoisomerase II inhibitor, which can cause DNA damage and induce apoptosis of tumour cells [53]. Imatinib, Sorafenib, Bosutinib and Sunitinib are tyrosine kinase inhibitors (TKIs) that are used in the treatment of many types of cancer [54]. The current standard first-line treatment for advanced ccRCC involves either an immuno-oncology (IO)/TKI or IO/IO combination [55]. Given the differences in immune cell infiltration, immune checkpoint expression, TIDE scores, and drug sensitivity between the high- and low-risk groups, a personalized treatment approach should be considered. For high-risk patients, although they have a higher risk of immune escape, a combination of immune checkpoint blockade and TKIs may be a viable option. The TKIs can not only inhibit tumour growth, but also potentially modulate the tumour microenvironment to enhance the anti-tumour effect of immunotherapy. In clinical practice, this risk score model provides doctors with an intuitive and quantitative tool that may be useful in assessing the risk of the condition in patients with ccRCC. By calculating the risk score, it helps doctors distinguish between high- and low-risk patients, and then formulate more personalized treatment plans. Future studies are needed to further validate these findings and optimize the treatment strategies for ccRCC patients in different risk groups.

There are some limitations in this study. Firstly, the specific molecular mechanism of model lncRNAs in ccRCC is still unclear and needs to be further clarified in subsequent studies. Secondly, a large number of real-world clinical data need to be collected to verify the constructed prognostic model. In conclusion, a novel prognostic model was constructed based on four DElncRNAs-related to DDR. The model has satisfactory accuracy in predicting survival of ccRCC patients. In addition, the clinical features, TMB, immune cell infiltration, immune checkpoint expression, and drug sensitivity of ccRCC patients in the high- and low-risk group were analysed, which provides new perspective for the study of the treatment of ccRCC patients and lays a foundation for future exploration of the molecular mechanism of ccRCC.

Acknowledgements

Not applicable. Conception and design: Renli Tian
Administrative support: Renli Tian
Provision of study materials or samples: Renli Tian
Collection and assembly of data: Peng Chen
Data analysis and interpretation: Jian Li
All authors have made important contributions to data analysis, drafting the article or revising the article. All authors have read and approved the final work.

Authors' contributions

CRedit: **Peng Chen**: Data curation; **Jian Li**: Data curation; **Renli Tian**: Conceptualization.

Ethics approval and consent to participate

This study was approved by the Ethics Committee of General Hospital of Northern Theater Command (Y(2024)277). This study complied with the Declaration of Helsinki. Written informed consent was obtained from all participants.

Consent for publication

Not applicable.

Disclosure statement

No potential conflict of interest was reported by the author(s).

Availability of data and materials

The RNA-seq data, matched survival information and clinicopathological features of The Cancer Genome Atlas-ccRCC (TCGA-ccRCC) were extracted from the University of California Sisha Cruz (UCSC) Xena database (<https://xena.ucsc.edu/>). The data generated during and/or analysed during the current study are available from the corresponding author on reasonable request.

Funding

This study was funded by the Natural Science Foundation of Liaoning Province (2022-MS-047).

References

- [1] Wang J, Jin J, Liang Y, et al. miR-21-5p/PRKCE axis implicated in immune infiltration and poor prognosis of kidney renal clear cell carcinoma. *Front Genet.* 2022;13:978840. doi: [10.3389/fgene.2022.978840](https://doi.org/10.3389/fgene.2022.978840).
- [2] Pan Q, Li F, Ding Y, et al. ORC6 acts as a biomarker and reflects poor outcome in clear cell renal cell carcinoma. *J Cancer.* 2022;13(8):2504–2514. doi: [10.7150/jca.71313](https://doi.org/10.7150/jca.71313).
- [3] Jiang H, Chen H, Wan P, et al. Decreased expression of HADH is related to poor prognosis and immune infiltration in kidney renal clear cell carcinoma. *Genomics.* 2021;113(6):3556–3564. doi: [10.1016/j.ygeno.2021.08.008](https://doi.org/10.1016/j.ygeno.2021.08.008).
- [4] Sun Z, Jing C, Guo X, et al. Comprehensive analysis of the immune infiltrates of pyroptosis in kidney renal clear cell carcinoma. *Front Oncol.* 2021;11:716854. doi: [10.3389/fonc.2021.716854](https://doi.org/10.3389/fonc.2021.716854).
- [5] Liu Y, Qu HC, Huang Y. Renal clear cell carcinoma-derived CXCL5 drives tumor-associated fibroblast formation and facilitates cancer progression. *Pathol Res Pract.* 2023;244(154319). doi: [10.1016/j.prp.2023.154319](https://doi.org/10.1016/j.prp.2023.154319).
- [6] Hsieh JJ, Purdue MP, Signoretti S, et al. Renal cell carcinoma. *Nat Rev Dis Primers.* 2017;3(1):17009. doi: [10.1038/nrdp.2017.9](https://doi.org/10.1038/nrdp.2017.9).
- [7] Comprehensive molecular characterization of clear cell renal cell carcinoma. *Nature.* 2013;499(7456):43–49. doi: [10.1038/nature12222](https://doi.org/10.1038/nature12222).
- [8] Bergers G, Hanahan D. Modes of resistance to anti-angiogenic therapy. *Nat Rev Cancer.* 2008;8(8):592–603. doi: [10.1038/nrc2442](https://doi.org/10.1038/nrc2442).
- [9] Carusillo A, Mussolino C. DNA damage: from threat to treatment. *Cells.* 2020;9(7):1665. doi: [10.3390/cells9071665](https://doi.org/10.3390/cells9071665).
- [10] Chatterjee N, Walker GC. Mechanisms of DNA damage, repair, and mutagenesis. *Environ Mol Mutagen.* 2017;58(5):235–263. doi: [10.1002/em.22087](https://doi.org/10.1002/em.22087).
- [11] Sun W, Zhang Q, Wang R, et al. Targeting DNA damage repair for immune checkpoint inhibition: mechanisms and potential clinical applications. *Front Oncol.* 2021;11:648687. doi: [10.3389/fonc.2021.648687](https://doi.org/10.3389/fonc.2021.648687).
- [12] He C, Kawaguchi K, Toi M. DNA damage repair functions and targeted treatment in breast cancer. *Breast Cancer.* 2020;27(3):355–362. doi: [10.1007/s12282-019-01038-2](https://doi.org/10.1007/s12282-019-01038-2).
- [13] Ged Y, Chaim JL, DiNatale RG, et al. DNA damage repair pathway alterations in metastatic clear cell renal cell carcinoma and implications on systemic therapy. *J Immunother Cancer.* 2020;8(1):e000230. doi: [10.1136/jitc-2019-000230](https://doi.org/10.1136/jitc-2019-000230).
- [14] Zhang ZY, Xu JH, Zhang JL, et al. CD276 enhances sunitinib resistance in clear cell renal cell carcinoma by promoting DNA damage repair and activation of FAK-MAPK signaling pathway. *BMC Cancer.* 2024;24(1):650. doi: [10.1186/s12885-024-12402-7](https://doi.org/10.1186/s12885-024-12402-7).
- [15] Schmitz SU, Grote P, Herrmann BG. Mechanisms of long noncoding RNA function in development and disease. *Cell Mol Life Sci.* 2016;73(13):2491–2509. doi: [10.1007/s00018-016-2174-5](https://doi.org/10.1007/s00018-016-2174-5).
- [16] Bhan A, Soleimani M, Mandal SS. Long noncoding RNA and cancer: a new paradigm. *Cancer Res.* 2017;77(15):3965–3981. doi: [10.1158/0008-5472.can-16-2634](https://doi.org/10.1158/0008-5472.can-16-2634).
- [17] Liu R, Zhang Q, Shen L, et al. Long noncoding RNA Inc-RI regulates DNA damage repair and radiation sensitivity of CRC cells through NHEJ pathway. *Cell Biol Toxicol.* 2020;36(5):493–507. doi: [10.1007/s10565-020-09524-6](https://doi.org/10.1007/s10565-020-09524-6).
- [18] Zhao S, Yu N, Wang H, et al. Long non-coding RNA PANDAR promoted radiation and cisplatin-induced DNA damage repair through ATR/CHK1 in NSCLC. *J Gene Med.* 2023;25(12):e3565. doi: [10.1002/jgm.3565](https://doi.org/10.1002/jgm.3565).
- [19] Su M, Wang H, Wang W, et al. LncRNAs in DNA damage response and repair in cancer cells. *Acta Biochim Biophys Sin (Shanghai).* 2018;50(5):433–439. doi: [10.1093/abbs/gmy022](https://doi.org/10.1093/abbs/gmy022).
- [20] Zheng XL, Zhang YY, Lv WG. Long noncoding RNA ITGB1 promotes migration and invasion of clear cell renal cell carcinoma by downregulating Mcl-1. *Eur Rev Med Pharmacol Sci.* 2023;27(3):834. doi: [10.26355/eur-rev_202302_31171](https://doi.org/10.26355/eur-rev_202302_31171).

- [21] Tang Z, Tang C, Sun C, et al. Long noncoding RNA-LINC00478 promotes the progression of clear cell renal cell carcinoma through PBX3. *J Biochem Mol Toxicol.* 2022;36(12):e23214. doi: [10.1002/jbt.23214](https://doi.org/10.1002/jbt.23214).
- [22] Wu H, Wu H, Sun P, et al. Effect of aberrant long noncoding RNA on the prognosis of clear cell renal cell carcinoma. *Comput Math Methods Med.* 2021;2021:6533049. doi: [10.1155/2021/6533049](https://doi.org/10.1155/2021/6533049).
- [23] Liu P, Deng X, Zhou H, et al. Multi-omics analyses unravel DNA damage repair-related clusters in breast cancer with experimental validation. *Front Immunol.* 2023;14:1297180. doi: [10.3389/fimmu.2023.1297180](https://doi.org/10.3389/fimmu.2023.1297180).
- [24] Huang H, Chen K, Zhu Y, et al. A multi-dimensional approach to unravel the intricacies of lactylation related signature for prognostic and therapeutic insight in colorectal cancer. *J Transl Med.* 2024;22(1):211. doi: [10.1186/s12967-024-04955-9](https://doi.org/10.1186/s12967-024-04955-9).
- [25] Flippot R, Beinse G, Boilève A, et al. Long non-coding RNAs in genitourinary malignancies: a whole new world. *Nat Rev Urol.* 2019;16(8):484–504. doi: [10.1038/s41585-019-0195-1](https://doi.org/10.1038/s41585-019-0195-1).
- [26] Zhang Y, Wang DL, Yan HY, et al. Genome-wide study of ER-regulated lncRNAs shows AP000439.3 may function as a key regulator of cell cycle in breast cancer. *Oncol Rep.* 2017;38(5):3227–3237. doi: [10.3892/or.2017.5975](https://doi.org/10.3892/or.2017.5975).
- [27] Sun Z, Wang J, Fan Z, et al. Investigating the prognostic role of lncRNAs associated with disulfidptosis-related genes in clear cell renal cell carcinoma. *J Gene Med.* 2024;26(1):e3608. doi: [10.1002/jgm.3608](https://doi.org/10.1002/jgm.3608).
- [28] Cao Y, Jiao N, Sun T, et al. CXCL11 correlates with anti-tumor immunity and an improved prognosis in colon cancer. *Front Cell Dev Biol.* 2021;9:646252. doi: [10.3389/fcell.2021.646252](https://doi.org/10.3389/fcell.2021.646252).
- [29] Liu K, Lai M, Wang S, et al. Construction of a CXC chemokine-based prediction model for the prognosis of colon cancer. *Biomed Res Int.* 2020;2020:6107865. doi: [10.1155/2020/6107865](https://doi.org/10.1155/2020/6107865).
- [30] Junnila S, Kokkola A, Mizuguchi T, et al. Gene expression analysis identifies over-expression of CXCL1, SPARC, SPP1, and SULF1 in gastric cancer. *Genes Chromosomes Cancer.* 2010;49(1):28–39. doi: [10.1002/gcc.20715](https://doi.org/10.1002/gcc.20715).
- [31] Noonan FC, Goodfellow PJ, Staloch LJ, et al. Antisense transcripts at the EMX2 locus in human and mouse. *Genomics.* 2003;81(1):58–66. doi: [10.1016/s0888-7543\(02\)00023-x](https://doi.org/10.1016/s0888-7543(02)00023-x).
- [32] Chen H, Pan Y, Jin X, et al. Identification of a four hypoxia-associated long non-coding rna signature and establishment of a nomogram predicting prognosis of clear cell renal cell carcinoma. *Front Oncol.* 2021;11:713346. doi: [10.3389/fonc.2021.713346](https://doi.org/10.3389/fonc.2021.713346).
- [33] Cao H, Tong H, Zhu J, et al. A glycolysis-based long non-coding RNA signature accurately predicts prognosis in renal carcinoma patients. *Front Genet.* 2021;12:638980. doi: [10.3389/fgene.2021.638980](https://doi.org/10.3389/fgene.2021.638980).
- [34] Jiang H, Chen H, Wan P, et al. Downregulation of enhancer RNA EMX2OS is associated with poor prognosis in kidney renal clear cell carcinoma. *Aging (Albany NY).* 2020;12(24):25865–25877. doi: [10.18632/aging.202151](https://doi.org/10.18632/aging.202151).
- [35] Wang Z, Zhang C, Chang J, et al. LncRNA EMX2OS, Regulated by TCF12, interacts with FUS to regulate the proliferation, migration and invasion of prostate cancer cells through the cGMP-PKG signaling pathway. *Onco Targets Ther.* 2020;13:7045–7056. doi: [10.2147/ott.s243552](https://doi.org/10.2147/ott.s243552).
- [36] Zeng H, Zhou S, Cai W, et al. LncRNA SNHG1: role in tumorigenesis of multiple human cancers. *Cancer Cell Int.* 2023;23(1):198. doi: [10.1186/s12935-023-03018-1](https://doi.org/10.1186/s12935-023-03018-1).
- [37] Tian P, Wei JX, Li J, et al. LncRNA SNHG1 regulates immune escape of renal cell carcinoma by targeting miR-129-3p to activate STAT3 and PD-L1. *Cell Biol Int.* 2021;45(7):1546–1560. doi: [10.1002/cbin.11595](https://doi.org/10.1002/cbin.11595).
- [38] Pei X, Wang X, Li H. LncRNA SNHG1 regulates the differentiation of Treg cells and affects the immune escape of breast cancer via regulating miR-448/IDO. *Int J Biol Macromol.* 2018;118(Pt A):24–30. doi: [10.1016/j.ijbio-mac.2018.06.033](https://doi.org/10.1016/j.ijbio-mac.2018.06.033).
- [39] Zhao S, Wang Y, Luo M, et al. Long noncoding RNA small nucleolar RNA host gene 1 (SNHG1) promotes renal cell carcinoma progression and metastasis by negatively regulating miR-137. *Med Sci Monit.* 2018;24:3824–3831. doi: [10.12659/msm.910866](https://doi.org/10.12659/msm.910866).
- [40] Tian P, Wei J, Li J, et al. An oncogenic role of lncRNA SNHG1 promotes ATG7 expression and autophagy involving tumor progression and sunitinib resistance of renal cell carcinoma. *Cell Death Discov.* 2024;10(1):273. doi: [10.1038/s41420-024-02021-3](https://doi.org/10.1038/s41420-024-02021-3).
- [41] Jackson SP, Bartek J. The DNA-damage response in human biology and disease. *Nature.* 2009;461(7267):1071–1078. doi: [10.1038/nature08467](https://doi.org/10.1038/nature08467).
- [42] Lord CJ, Ashworth A. The DNA damage response and cancer therapy. *Nature.* 2012;481(7381):287–294. doi: [10.1038/nature10760](https://doi.org/10.1038/nature10760).
- [43] Tiek D, Cheng SY. DNA damage and metabolic mechanisms of cancer drug resistance. *Cancer Drug Resist.* 2022;5(2):368–379. doi: [10.20517/cdr.2021.148](https://doi.org/10.20517/cdr.2021.148).
- [44] Torgovnick A, Schumacher B. DNA repair mechanisms in cancer development and therapy. *Front Genet.* 2015;6:157. doi: [10.3389/fgene.2015.00157](https://doi.org/10.3389/fgene.2015.00157).
- [45] Bell HN, Kumar-Sinha C, Mannan R, et al. Pathogenic ATM and BAP1 germline mutations in a case of early-onset, familial sarcomatoid renal cancer. *Cold Spring Harb Mol Case Stud.* 2022;8(3):a006203. doi: [10.1101/mcs.a006203](https://doi.org/10.1101/mcs.a006203).
- [46] Xin Z, Wen X, Zhou M, et al. Identification of molecular characteristics of FUT8 and alteration of core fucosylation in kidney renal clear cell cancer. *Aging (Albany NY).* 2024;16(3):2299–2319. doi: [10.18632/aging.205482](https://doi.org/10.18632/aging.205482).
- [47] Yin W, Wang JH, Liang YM, et al. Effects of purine metabolism-related LINC01671 on tumor heterogeneity in kidney renal clear cell carcinoma. *Front Biosci (Landmark Ed).* 2023;28(12):354. doi: [10.31083/j.fbl2812354](https://doi.org/10.31083/j.fbl2812354).
- [48] Arnoff TE, El-Deiry WS. CDKN1A/p21(WAF1), RB1, ARID1A, FLG, and HRNR mutation patterns provide insights into urinary tract environmental exposure carcinogenesis and potential treatment strategies. *Am J Cancer Res.* 2021;11(11):5452–5471.
- [49] Chen Y, Zhou X, Xie Y, et al. Establishment of a seven-gene signature associated with CD8(+). T Cells through the Utilization of Both Single-Cell and Bulk RNA-Sequencing Techniques in Clear Cell Renal Cell Carcinoma. 2023;24(18):13729. doi: [10.3390/ijms241813729](https://doi.org/10.3390/ijms241813729).

- [50] Brech D, Herbstritt AS, Diederich S, et al. Dendritic cells or macrophages? the microenvironment of human clear cell renal cell carcinoma imprints a mosaic myeloid subtype associated with patient survival. *Cells*. 2022;11(20):3289. doi: [10.3390/cells11203289](https://doi.org/10.3390/cells11203289).
- [51] Braun DA, Street K, Burke KP, et al. Progressive immune dysfunction with advancing disease stage in renal cell carcinoma. *Cancer Cell*. 2021;39(5):632–648.e638. doi: [10.1016/j.ccell.2021.02.013](https://doi.org/10.1016/j.ccell.2021.02.013).
- [52] Xue B, Guo WM, Jia JD, et al. MUC20 as a novel prognostic biomarker in ccRCC correlating with tumor immune microenvironment modulation. *Am J Cancer Res*. 2022;12(2):695–712.
- [53] Jang JY, Kim D. Etoposide as a key therapeutic agent in lung cancer: mechanisms. Efficacy, and Emerging Strategies. 2025;26(2):796. doi: [10.3390/ijms26020796](https://doi.org/10.3390/ijms26020796).
- [54] Braun D, Kim TD, Le Coutre P, et al. Tyrosine kinase inhibitors noncompetitively inhibit MCT8-mediated iodothyronine transport. *J Clin Endocrinol Metab*. 2012;97(1):E100–105. doi: [10.1210/jc.2011-1837](https://doi.org/10.1210/jc.2011-1837).
- [55] Chen YW, Rini BI, Beckermann KE. Emerging targets in clear cell renal cell carcinoma. *Cancers (Basel)*. 2022;14(19):4843. doi: [10.3390/cancers14194843](https://doi.org/10.3390/cancers14194843).